PHYSICAL MODELLING OF THE ZIRCONIUM ALLOY TUBE PILGER ROLLING PROCESS

DYJA Henryk[1], KAWAŁEK Anna[1], OZHMEGOV Kirill[2], SAWICKI Sylwester[1], LABER Konrad[1]

[1]*Czestochowa University of Technology, Faculty of Production Engineering and Materials Technology, Institute for Plastic Working and Safety Engineering, Czestochowa, Poland, EU, dyja.henryk@wip.pcz.pl*

[2]*National University of Science and Technology "MISIS" (MISIS), Moscow, Russian Federation, pdss@misis.ru*

Abstract

The paper presents the results of investigation concerned with the inner surface quality of Zr-1% Nb alloy tubes produced on a KPW-type pilger rolling mill with an elongation factor of λ = 3.9. In order to analyze the influence of applied velocities and deformations on the variations of the flow stress σ_p values of the investigated alloy, an experiment by testing programme was carried out in industrial conditions and the physical modelling of the rolling process was performed. For the physical modelling of the investigated process, the metallurgical process simulator GLEEBLE 3800 was employed. The relationships $\sigma_p = \sigma_p(\varepsilon, \dot{\varepsilon})$ have been obtained for the conditions of both intermittent and continuous cold deformation of the examined alloy and recommendations for the distribution of stress across the rolling gap have been given.

Keywords: Pilger rolling, zirconium alloy, tube inner surface defects, flow stress, physical modelling

1. INTRODUCTION

The intensification of the plastic working process of zirconium-based alloys by reducing the number of operations during the tube cold rolling on pilger rolling mill may lead to decrease of the quality of the outer and inner surfaces of semi-finished products and tubes. After shortening duration of the technological process, the occurrence of defects from rolling was observed after all cold plastic working cycles; discontinuities forming due to metal sticking to the rolls and the formation of a fatigue crack were disclosed, and increased surface roughness and the formation of a varying tube profile, etc., were noticed.

The optimization of tube cold rolling technology and other technological processes [1] requires a detailed analysis of all interacting physical processes. The analysis and physical modelling of variable-load processes, in the case of tube cold rolling, are relatively complex due to the fact that the behaviour and value of the flow stress σ_p in the plastic flow curves σ_p - ε for zirconium alloys are influenced by a number of conditions and parameters [2-4]. Among them, the following should be mentioned: the distribution of strain across length of the deformation zone, the value of the total deformation during the complete rolling cycle, the distribution of strain rate and the occurrence of the plastic deformation thermal effect during the tube rolling.

The influence and interactions of these parameters can be noticed by carrying out the experimental physical modelling of the intermittent loading process under conditions similar to the tubes rolling on KPW pilger rolling mill using modern plastometric testing machine [5-7].

2. THE AIM, SCOPE AND METHODOLOGY OF THE INVESTIGATION

The purpose of the investigation was to identify the causes of the defects formation on the inner tube surface and to determine the influence of cold pilger rolling conditions on the variations of the flow stress σ_p values of the Zr-1% Nb alloy during growing tube deformation in the roll gap.

To identify the causes of the defects forming on the inner surface of products, sections of the metal from the deformation zone (working cone) were taken from the tube length being rolled and examinations were made to determine the inner surface quality using an optical microscope at a magnification of 10x and 1000x, respectively. The analysis of the rolling process parameters was made using the «Gleeble 3800» metallurgical process simulator in the «Pocket Jaw» module, according to the testing methodology described in works [8, 9]. Prior to physical modelling, the influence of rolling conditions on the flow stress values of the Zr-1% Nb alloy was determined. Specimens with a working portion diameter of 10 mm and a height to 12 cm made from 14 mm-diameter bars were used for the tests. The state of the alloy after the cold deformation and annealing could be defined as completely recrystallized with a grain size of 9-10 according to the standard scale [10]. The tests were performed by the compression method following the intermittent loading schemes shown in **Table 1**, and also under continuous loading conditions within the velocity range of 0.5 -15.0 s^{-1}. The temperature of the deformed specimens was monitored using chromel-copel thermocouples that were welded in the central specimen portion by a „Thermocouple Welder" welding machine. It made possible not only controling the temperature of heated alloy, but also recording variations of the value of the plastic deformation thermal effect (PDTE) - the temperature change ΔT during testing. As the lubricant, graphite-based pads were used.

Table 1 Deformation parameters in modelling of Zr-1% Nb alloy tube rolling

Scheme 1		
Pass	Strain ε (-)	Strain rate $\dot{\varepsilon}$ (1/s)
1	0.13	3.1
2	0.11	2.9
3	0.09	2.8
4	0.08	2.7
5	0.07	2.6
6	0.06	2.6
7	0.05	2.5
8	0.04	2.4
9	0.03	2.3
10	0.03	2.2
11	0.02	2.1
12	0.02	1.9
13	0.02	1.8
14	0.01	1.7
15	0.01	1.6
16	0.01	1.4
17	0.01	1.3
18	0.01	1.1
19	0.01	0.9
Break time after deformation, t = 2.4 s		

Scheme 2		
Pass	Strain ε (-)	Strain rate $\dot{\varepsilon}$ (1/s)
1	0.11	3.1
2	0.10	2.9
3	0.08	2.8
4	0.07	2.7
5	0.06	2.6
6	0.05	2.6
7	0.05	2.5
8	0.04	2.4
9	0.04	2.3
10	0.03	2.2
11	0.03	2.1
12	0.02	1.9
13	0.02	1.8
14	0.02	1.7
15	0.02	1.6
16	0.01	1.4
17	0.01	1.3
18	0.01	1.1
19	0.01	0.9
Break time after deformation, t = 2.4 s		

Scheme 3		
Pass	Strain ε (-)	Strain rate $\dot{\varepsilon}$ (1/s)
1	0.02	0.9
2	0.02	1.1
3	0.02	1.3
4	0.03	1.4
5	0.03	1.6
6	0.03	1.7
7	0.04	1.8
8	0.04	1.9
9	0.04	2.1
10	0.04	2.2
11	0.04	2.3
12	0.05	2.4
13	0.05	2.5
14	0.05	2.6
15	0.05	2.6
16	0.05	2.7
17	0.06	2.8
18	0.06	2.9
19	0.06	3.1
20	0.08	4.1
Break time after deformation, t = 2.4 s		

Scheme 4		
Pass	Strain ε (-)	Strain rate $\dot{\varepsilon}$ (1/s)
1	0.12	3.0
2	0.11	2.8
3	0.10	2.6
4	0.09	2.4
5	0.09	2.2
6	0.08	2.0
7	0.07	1.8
8	0.06	1.5
9	0.05	1.2
10	0.02	0.9
Break time after deformation, t = 4.8 s		

Figure 1 illustrates the strain distributions corresponding to the specimen loading schemes (**Table 1**). The schemes describe the variation of strain rate and strain across the deformation zone in the KPW pilger rolling mill. Schemes 1, 2 and 4 correspond to the values of the total specimen deformation of $\Sigma\varepsilon$ = 0.65 and the decreasing values of strain along the roll gap at the end of loading.

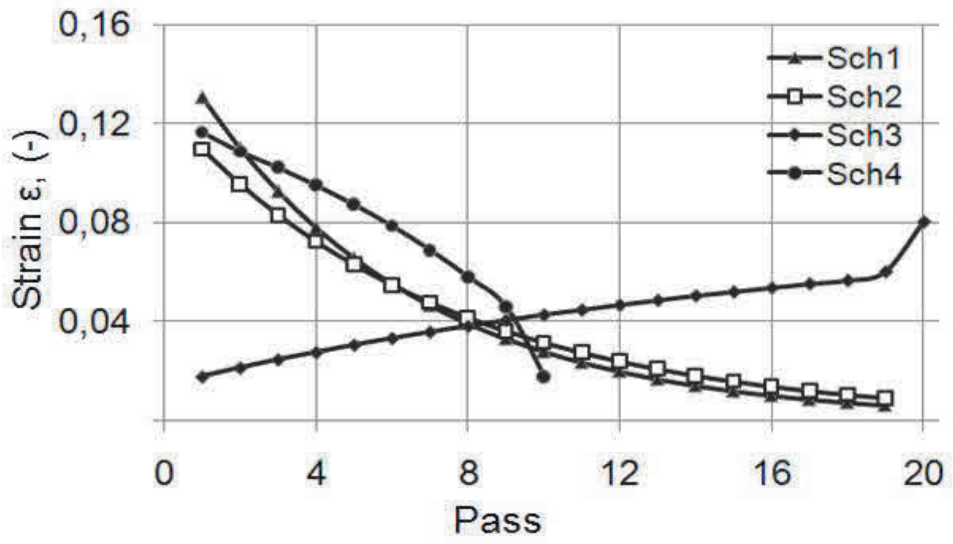

Figure 1 The strain distribution for different schemes of tube loading in the pass

Deformation scheme no. 3 applies to the total specimen deformation of $\Sigma\varepsilon$ = 0.69 and describes the distribution of rolling reductions increasing in the final loading cycle phase. Scheme 4 is characterized by a more intensive strain with the total specimen deformation of $\Sigma\varepsilon$ = 0.65 being attained within 10 tube loadings. For a given scheme, the break between loadings increased from 2.4 s (for schemes 1-3) to 4.8 s. Scheme 4 represents rolling simulation with a greater tube advance in the deformation zone and a decreased frequency of working roll displacement, compared to the other schemes.

3. ANALYSIS OF THE INVESTIGATION RESULTS

3.1. The results of the examination of the working cone inner surface

To assess the influence of the conditions of tube deformation according to different technological schemes, the rolling process was stopped and sections of blanks containing the material occurring in the working cone during the pilger process were taken. Many defects were found on the inner surface of the blank section (**Figure 2**), which number and size increased with increasing the deformation value applied during the rolling process (**Figure 3**).

Figure 2 The appearance of the inner surface of a blank taken from the working cone during the rolling of Zr-1% Nb alloy on the KPW pilger rolling mill

In the initial portion of working cone (**Figure 3a**), the inner surface of a blank is mostly uniform, with its roughness being *Ra* ≈ 0.2 - 0.3. The helical path visible over the whole tube working cone length is a remnant from the previous working tool contact with the inner surface of tube. Micro-cracks formed with a depth ranging from 1 to 3 μm, oriented to the tube axis at an angle of 45-60°, are visible on the specimens **(Figures 3b, 4a**). The distance between crack boundaries does not exceed 1 μm. With the increase of preset deformation, a change in the micro-crack development direction and the formation of new micro-cracks with a width of up to 3 μm were noticed (**Figures 3c, 3d; 4b, 4c**). Whereas, the micro-crack formation process is continuous and takes place along the deformation zone. It should be noted that the micro-crack development occurs chiefly directly on already formed defects or in a close distance from them. In the last portion of working cone (**Figure 3e**), the fatigue cracks attain a width of up to 150 μm and a depth of up to 15 μm (**Figure 4d**). The surface roughness *Ra* on the inner surface of a tube at the deformation zone ranges from 0.5 to 0.9.

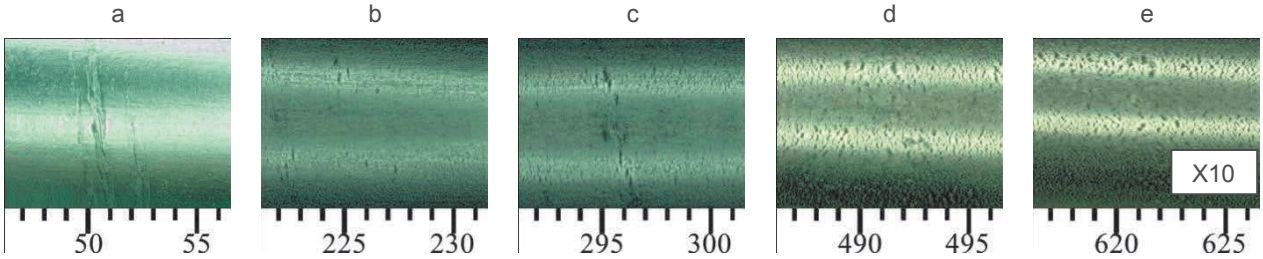

Figure 3 Variations of micro-cracks quantify and size on the inner surface of a tube made of Zr-1% Nb alloy across the deformation zone during the rolling on the KPW pilger rolling mill

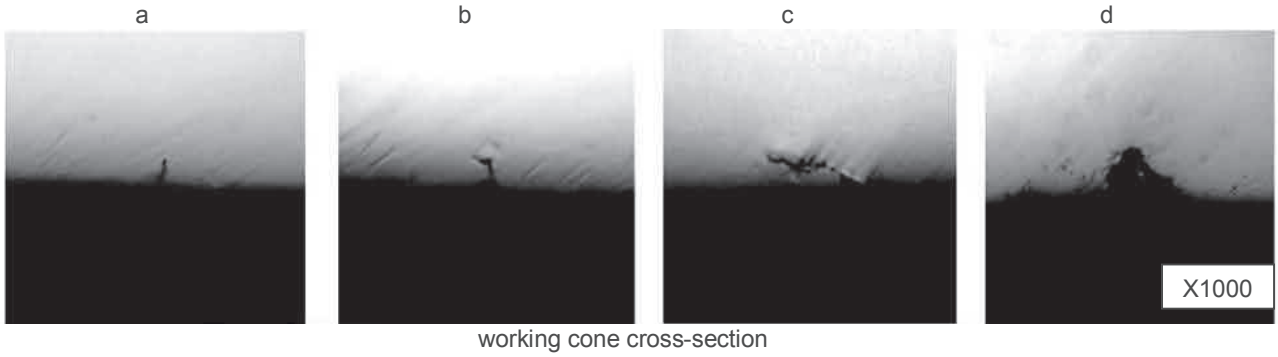

Figure 4 Fatigue crack-type defects on the inner surface of a tube taken from the working cone in the deformation zone during the rolling on the KPW pilger rolling mill

The formation of defects on the inner surface is a result of the increase of the permissible value of limiting strains for the Zr-1% Nb alloy under the conditions of suboptimal friction between the working tool and the rolled metal [11]. For these reasons, the problem of improving the surface quality can be solved by determining the rolling parameters responsible for attaining the indicated strain state with lower values of the flow stress σ_P and the friction coefficient μ.

3.2. The results of physical modelling of the influence of rolling conditions on the magnitude of the flow stress σ_P of the Zr-1% Nb alloy

Figure 5 shows σ_P - ε plastic flow curves for the Zr-1% Nb alloy obtained under intermittent loading conditions of the specimen according to schemes 1 and 3. It can be noticed from the curves that with strains of up to ε = 0.3, the value of the flow stress σ_P increases to 900 MPa. With the continued increase of strain ε > 0.3, the

value of σ_P stabilizes in the range of 900-1050 MPa. The maximum value in the σ_P - ε flow curves for scheme 1 is slightly shifted towards smaller strains. Increasing the single deformations ε to 0.08 at a strain rate of $\dot{\varepsilon}$ = 4.1 s^{-1} in the final loading cycle and the total deformation value to $\Sigma\varepsilon \approx 0.69$, according to scheme 3, has not influenced the value of σ_P.

Most probably, under cold deformation conditions with strains $\varepsilon > 0.3$, the stress attains values sufficiently high for the formation of cross slip bands [9, 12]. In that case, rebuilding of the entire dislocation structure and some reduction of lattice defects occur. Reactions between dislocations with opposite signs were observed, which manifested itself by their mutual cancellation and a reduction of the internal stress field. As a result of the increase of deformation, a gradual reduction of work hardening factor value occurs. Besides, the zirconium alloys are characterized by instability in plastic flow [13-15]. This phenomenon manifests itself in a parabolic shape of the plastic flow curve with the change in the local stress distribution in time and accompanies the periodical stress build-up in the form of stable macro-location zones, from which the specimen assumes a barrel-shaped form upon the compression conditions.

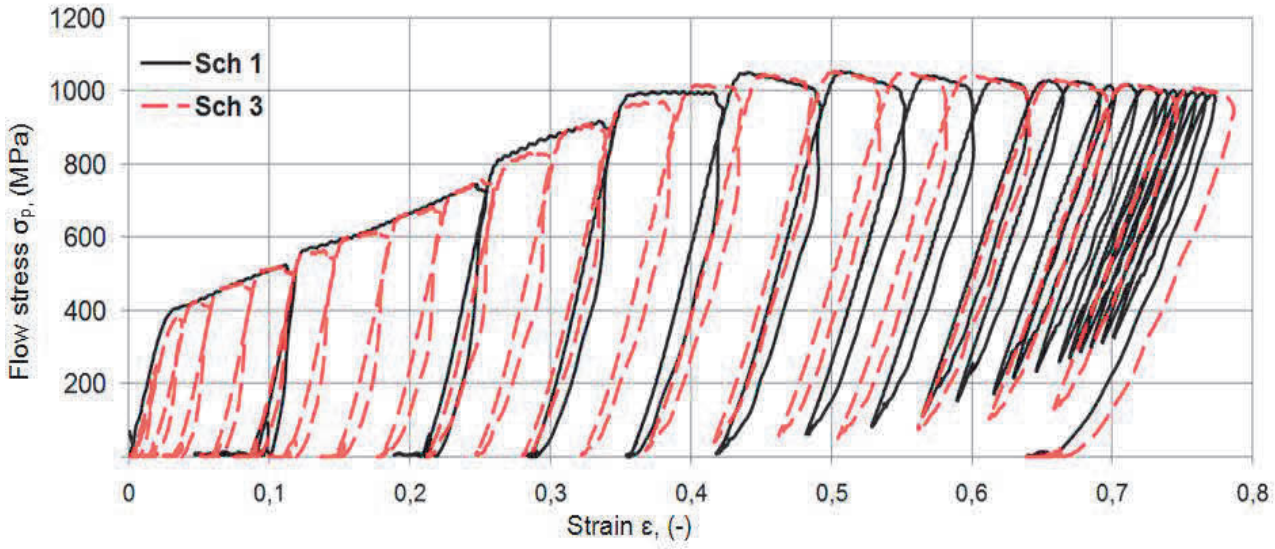

Figure 5 The σ_P - ε plastic flow curves for the Zr-1% Nb alloy obtained under intermittent loading conditions of the specimen in the Gleeble 3800 simulator according to schemes 1 and 3

When examining the plastic deformation thermal effect it was found that the temperature increase of specimens deformed according to schemes 1 and 3 did not exceed ΔT_{max} = 50 °C. Moreover, for the specimen deformed according to scheme 1, the ΔT_{max} value was shifted towards smaller strains of ε = 0.2-0.4.

Figure 6 shows σ_P - ε flow curves for the Zr-1% Nb alloy obtained under intermittent loading conditions of specimen according to schemes 2 and 4. The strain redistribution, according to scheme 4, provides a total specimen deformation of $\Sigma\varepsilon \approx 0.69$ in 10 loading steps, with the value of the flow stress σ_P being slightly lower than for specimen deformation according to scheme 2. In the ε strain range from 0.2 to 0.65, the value of $\Delta\sigma_P$ is about 60 MPa. The decrease of the σ_P value can be explained by the increasing PDTE value. When loading the specimen according to scheme 4, the ΔT_{max} is 80 °C and occurs in the strain range from 0.3 to 0.5. According to scheme 2, the ΔT_{max} value is 50 °C and is shifted towards strains with smaller values of ε = 0.15-0.4.

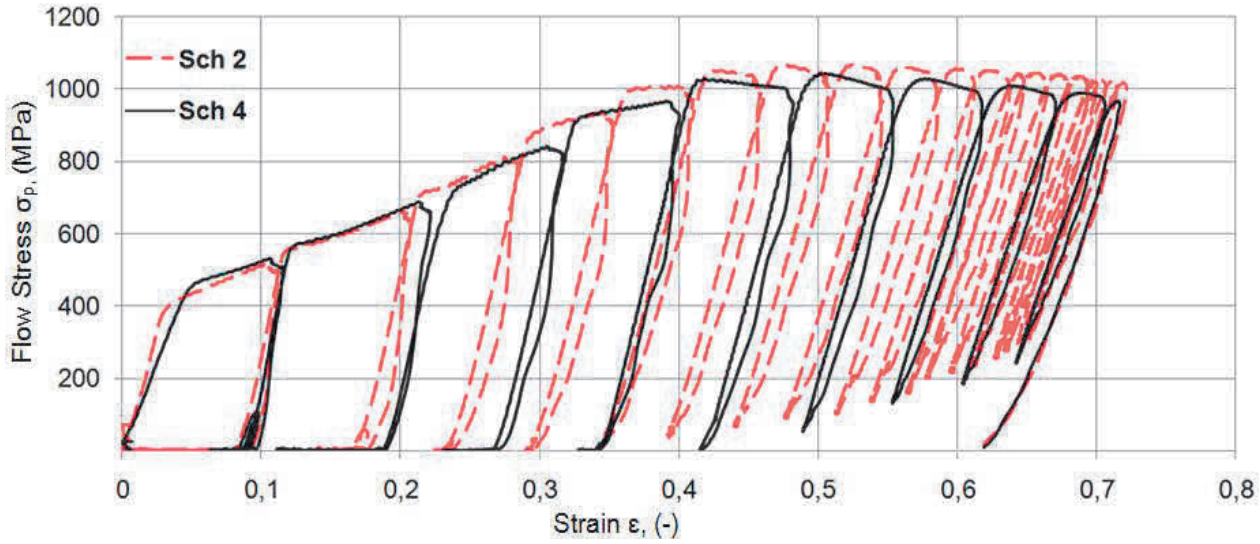

Figure 6 The σ_P - ε plastic flow curves for the Zr-1% Nb alloy obtained under intermittent loading conditions of the specimen in the Gleeble 3800 simulator according to schemes 2 and 4.

Figure 7 shows σ_P - ε plastic flow curves for the Zr-1% Nb alloy, obtained under continuous loading conditions of the specimen for the strain rate $\dot{\varepsilon}$ within the range of 0.5-15 s^{-1}. For this $\dot{\varepsilon}$ range, the specimen deformation starts at flow stress values of σ_P = 400-500 MPa, and up to a strain of $\varepsilon \approx 0.25$ it proceeds at a constant strain hardening factor. At strains of $\varepsilon > 0.25$, the strain hardening factor decreases. It should be noted that with the increase in the strain rate $\dot{\varepsilon}$ to 15 s^{-1}, the difference in σ_P flow stress values decreases. This might be due to the increasing PDTE influence on the flow stress values. At a strain rate of $\dot{\varepsilon}$ = 0.5 s^{-1} the value of the plastic deformation thermal effect is $\Delta T \approx 110$ °C, and at $\dot{\varepsilon}$ = 5 s^{-1}, the PDTE is equal to $\Delta T \approx 130$ °C, while at $\dot{\varepsilon}$ = 15 s^{-1} the PDTE equals $\Delta T \approx 150$ °C.

Comparison of the intermittent and continuous loading curves (for $\dot{\varepsilon}$ = 0.5 - 5 s^{-1}) for the Zr-1% Nb alloy shows that for strains of $\varepsilon \approx 0.2$ the σ_P flow stress values are comparable. At strains of $\varepsilon > 0.2$, the plastic flow curves obtained under intermittent loading conditions lie above the ones for continuous loading. The break between loading steps allows the PDTE influence on the σ_P flow stress value to be reduced.

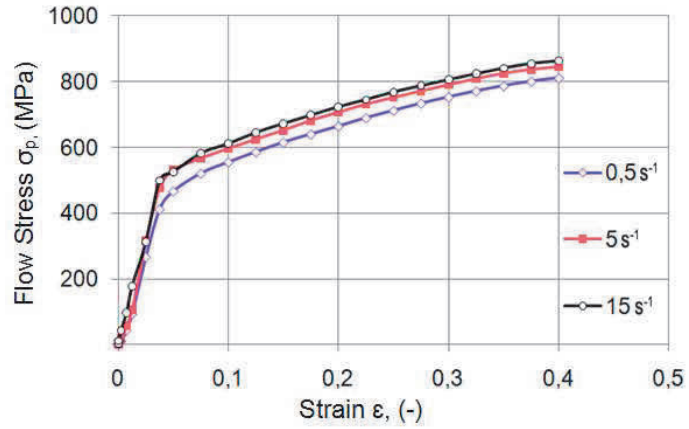

Figure 7 The σ_P - ε plastic flow curves for the Zr-1% Nb alloy at T = 20 °C, obtained under continuous loading conditions at a strain rate of 0.5, 5 and 15 s^{-1}, respectively.

The results shown in **Figures 5 - 7** indicate that the σ_P flow stress value under cold rolling conditions is influenced by numerous factors, including the $\dot{\varepsilon}$ strain rate, the value of preset ε plastic deformations in single operations, and the duration of breaks between preset loads. Increasing the strain rate results in intensified heating and a reduction of strain hardening factors of the alloy. To reduce the influence of the plastic deformation thermal effect, technological lubricants need to be used during deformation, which will reduce the friction occurring on the surfaces of contact between the tool and the rolled metal.

4. CONCLUSIONS

From the investigation carried out, the following findings and conclusions have been formulated:

- The analysis of the stages of formation and development of defects on the inner surface of tubes during their production on the pilger rolling mill has been made. Inner surface defects form as a result of the increase in the permissible value of the limiting strains of the Zr-1% Nb alloy under the conditions of suboptimal friction between the working tool and the rolled metal;
- Relationships for the Zr-1% Nb alloy between the σ_P flow stress and the strain rate parameters in intermittent and continuous loading conditions similar to those occurring in the process of cold tube production on the pilger rolling mill have been determined. It has been demonstrated that the intensification of the rolling process leads to an increase in the plastic deformation thermal effect and a reduction of the flow stress. The determined relationships for continuous loading can be used for description of the cold rolling process with strains of up to $\varepsilon \approx 0.2$.

REFERENCES

[1] LABER, K., DYJA, H., KALAMORZ, M. Analysis of the technology of rolling 5.5 mm-diameter wire rod of cold upsetting steel in the Morgan Block Mill. *Metalurgija*, 2015, vol. 54, no. 2, pp. 415-418.

[2] DYJA, H., KAWAŁEK, A., GALKIN, A. M., OZHMEGOV, K. V., SAWICKI, S. Physical modelling of the multi-pass forging of zirconium alloy blanks. In *METAL 2014. 23rd International Conference on Metallurgy and Materials*. Ostrava: TANGER, 2014, pp. 402-406.

[3] KRIVTSOVA, O., VIVENTSOV, A., TALMAZAN, V., PANIN, E., ARBUZ, A. Study of deformation`s indexes of rolls of diffetent designs. *Applied Mechanics and Materials*, 2013, vol. 378, pp. 394-396.

[4] POLUHIN, P.I., GUN, G.YA., GALKIN, A.M. *Soprotivlenie plasticheskoj deformacii metallov i splavov*. M.: Metallurgiya, 1983, 351 p. (in Russian).

[5] DEMBICZAK, T., KNAPINSKI, M., GARBARZ, B. Mathematical modeling of phenomena of dynamic recrystallization during hot plastic deformation in high-carbon bainitic steel. *Metalurgija*, 2017, vol. 56, no. 1-2, pp. 107-110.

[6] KRIVTSOVA, O., TALMAZAN, V., ARBUZ, A., SIVYAKOVA, G. Study the process of equal-channel angular pressing with quasi-ultra-small angles of joint channels using computer modeling in program complex DEFORM. *Advanced Materials Research*, 2014, vol. 1030-1032, pp. 1337-1341.

[7] NAIZABEKOV, A., TALMAZAN, V., ARBUZ, A., KOINOV, T., LEZHNEV, S. Study of axial forces with the purpose to realize a combined process «helical rolling-pressing». *Journal of Chemical Technology and Metallurgy*, 2015, vol. 50, no. 2, pp. 217-222.

[8] KAWAŁEK, A., DYJA, H.,GAŁKIN, A. M.,OZHMEGOV, K. V.,SAWICKI, S. Physical modelling of the plastic working processes of zirconium alloy bars and tubes in thermomechanical conditions. *Archives of Metallurgy and Materials*, 2014, vol. 59, no. 3, pp. 935-940.

[9] GAŁKIN, A. *Badania plastometryczne metali i stopów*. *Plastomeric studies of metals and alloys*. University Press of the Czestochowa University of Technology, Czestochowa 1990, p. 142. (in Polish).

[10] NIKULINA, A.V. Cirkonievye splavy v atomnoj ehnergetike. *Materialovedenie i termicheskaya obrabotka*, 2004, no. 11, pp. 8-12. (in Russian).

[11] GALKIN, A.M., NIKULIN, A.D., BOCHAROV, O.V. et al. *Cvetnye metally* 1997, no. 3, pp. 51-57. (in Russian).

[12] CHERNYAEVA, T.P., GRICINA, V.M. Harakteristiki GPU-metallov, opredelyayushchie ih povedenie pri mekhanicheskom, termicheskom i radiacionnom vozdejstvii. *Voprosy atomnoj nauki i tekhniki*, 2008, no. 2, pp. 15-27. (in Russian).

[13] POLETIKA, T. M. et al. Lokalizaciya plasticheskogo techeniya v splave Zr-l%Nb. *Zhurnal tekhnicheskoj fiziki*, 2002, vol. 72 ,no. 9, pp. 57-63. (in Russian).

[14] ZUEV, L. B., POLETIKA, T. M., NARIMANOVA, G. N. O svyazi mezhdu makrolokalizaciej plasticheskogo techeniya i dislokacionnoj strukturoj. *Pis'ma v zhurnal tekhnicheskoj fiziki*, 2003, vol. 29, no. 12, pp. 74-77. (in Russian).

[15] PSHENICHNIKOV, A. P. *Neustojchivost' plasticheskogo techenija v GPU splava cirkonija*. *Instability of plastic flow in h.c.p. zirconium alloy*. Tomsk 2010, 183 p. (in Russian).